THE JOURNAL OF BIOLOGICAL CHEMISTRY VOL. 282, NO. 17, pp. 12734–12740, April 27, 2007

Disruption of the GDNF Binding Site in NCAM Dissociates Ligand Binding and Homophilic Cell Adhesion*[S]

Received for publication, February 22, 2007 Published, JBC Papers in Press, February 23, 2007, DOI 10.1074/jbc.M701588200

Dan Sjöstrand[‡], Jonas Carlsson[§], Gustavo Paratcha[‡1], Bengt Persson[§¶], and Carlos F. Ibáñez[‡2]

From the [‡]Division of Molecular Neurobiology, Department of Neuroscience, and [¶]Department of Cell and Molecular Biology, Karolinska Institute, S-171 77 Stockholm, Sweden and [§]IFM Bioinformatics, Linköping University, S-581 83 Linköping, Sweden

Most plasma membrane proteins are capable of sensing multiple cell-cell and cell-ligand interactions, but the extent to which this functional versatility is founded on their modular design is less clear. We have identified the third immunoglobulin domain of the Neural Cell Adhesion Molecule (NCAM) as the necessary and sufficient determinant for its interaction with Glial Cell Line-derived Neurotrophic Factor (GDNF). Four charged contacts were identified by molecular modeling as the main contributors to binding energy. Their mutation abolished GDNF binding to NCAM but left intact the ability of NCAM to mediate cell adhesion, indicating that the two functions are genetically separable. The GDNF-NCAM interface allows complex formation with the GDNF family receptor α1, shedding light on the molecular architecture of a multicomponent GDNF receptor.

Members of the glial cell line-derived neurotrophic factor (GDNF)[3] family regulate cell survival, differentiation, and migration in the peripheral and central nervous systems as well as in a few peripheral organs. The four members of this ligand family, *i.e.* GDNF, Neurturin, Artemin, and Persephin, share ~40% of their amino acid sequence. GDNF and Artemin are being developed as therapeutic agents against Parkinson disease and peripheral neuropathies, respectively (1–3). Signaling by GDNF family ligands is mediated by alternative multicomponent receptor complexes containing a ligand binding, glycosylphosphatidylinositol-anchored subunit termed GDNF family receptor α (GFRα) (4–9), together with either the RET receptor tyrosine kinase (10, 11) or the neural cell adhesion molecule (NCAM) (12) as signaling subunits. Four related GFRα proteins, termed GFRα1 to 4, with different ligand specificity have been identified (13). In collaboration with RET, GFRα1 mediates the effects of GDNF on neuronal differentiation and migration in the developing enteric nervous system (14, 15) and ureter morphogenesis during kidney development (16, 17). On the other hand, in the presence of NCAM, GDNF and GFRα1 stimulate neurite outgrowth *in vitro* (12) and synaptogenesis *in vitro* and *in vivo* (18) in hippocampal neurons, stimulate migration of neuronal precursors in the rostral migratory stream (12, 19), and regulate Schwann cell migration and function (12, 20). Despite the importance of GDNF signaling for normal development and its possible therapeutic applications, the molecular architecture of these receptor complexes is not yet understood.

Crystal structures have been described for GDNF (21), a fragment of the ligand binding domain of GFRα1 (22), and the complex between Artemin and the ligand binding domain of its cognate GFRα3 receptor (23). The latter validated previous mutagenesis studies performed on GDNF ligands and GFRα receptors (24–26) and demonstrated that the ligand binding domain of GFRα receptors is formed by a single compact module that interacts with the poles of the elongated dimer of GDNF family ligands. In addition, a model of the extracellular region of RET based on four consecutive cadherin-like domains has been reported (27), but crystal structure data are still missing. The extracellular region of NCAM is composed of five immunoglobulin-like (Ig) and two fibronectin-like domains, and the crystal structure of the first three Ig domains has been reported (28).

Previous work has indicated that NCAM, unlike RET, can interact directly with GDNF but that high affinity binding and downstream signaling requires co-expression with the GDNF co-receptor GFRα1 (12). However, it has been unclear whether the ability of NCAM to bind GDNF is related to its adhesive properties or mediated by a distinct and specific protein-protein interaction interface. In this study, we set out to delineate GDNF binding determinants in NCAM and characterize their requirement for NCAM-mediated cell adhesion.

EXPERIMENTAL PROCEDURES

NCAM Deletion Constructs and Site-directed Mutagenesis

Domain boundaries in the rat NCAM[140] cDNA (Entrez ID X06564) (29) were defined based on the exon-intron structure of the chicken *Ncam* gene (Entrez ID AH005321) (30). The boundaries used for generation of *Ncam* deletion constructs were as follows (numbering refers to the mature protein, excluding the 19-residue signal peptide): domain 1, Leu[1]-Gln[97]; domain 2, Lys[98]-Val[191]; domain 3, Pro[192]-Ala[288]; domain 4,

* This work was supported by grants from the Swedish Foundation for Strategic Research, the Swedish Research Council (33X-10908-10A and 2004-6434), the Swedish Cancer Society (3474-B97-05XBC), the Vth Framework Program of the European Commission (QLG3-CT-2002-01000), the Karolinska Institute (to C. F. I.), and Linköping University (to B. P.). The costs of publication of this article were defrayed in part by the payment of page charges. This article must therefore be hereby marked "*advertisement*" in accordance with 18 U.S.C. Section 1734 solely to indicate this fact.

[S] The on-line version of this article (available at http://www.jbc.org) contains the coordinates of model in Fig. 2A.

[1] Supported by the Swedish Research Council. Currently affilited with the Laboratory of Molecular and Cellular Neuroscience, Dept. of Neuroscience, Karolinska Institute.

[2] To whom correspondence should be addressed. Tel.: 46-8-5248-7660; Fax: 46-8-33-95-48; E-mail: carlos.ibanez@ki.se.

[3] The abbreviations used are: GDNF, glial cell line-derived neurotrophic factor; GFRα, GDNF family receptor α; NCAM, neural cell adhesion molecule; HA, hemagglutinin; Ig, immunoglobulin; PBS, phosphate-buffered saline.

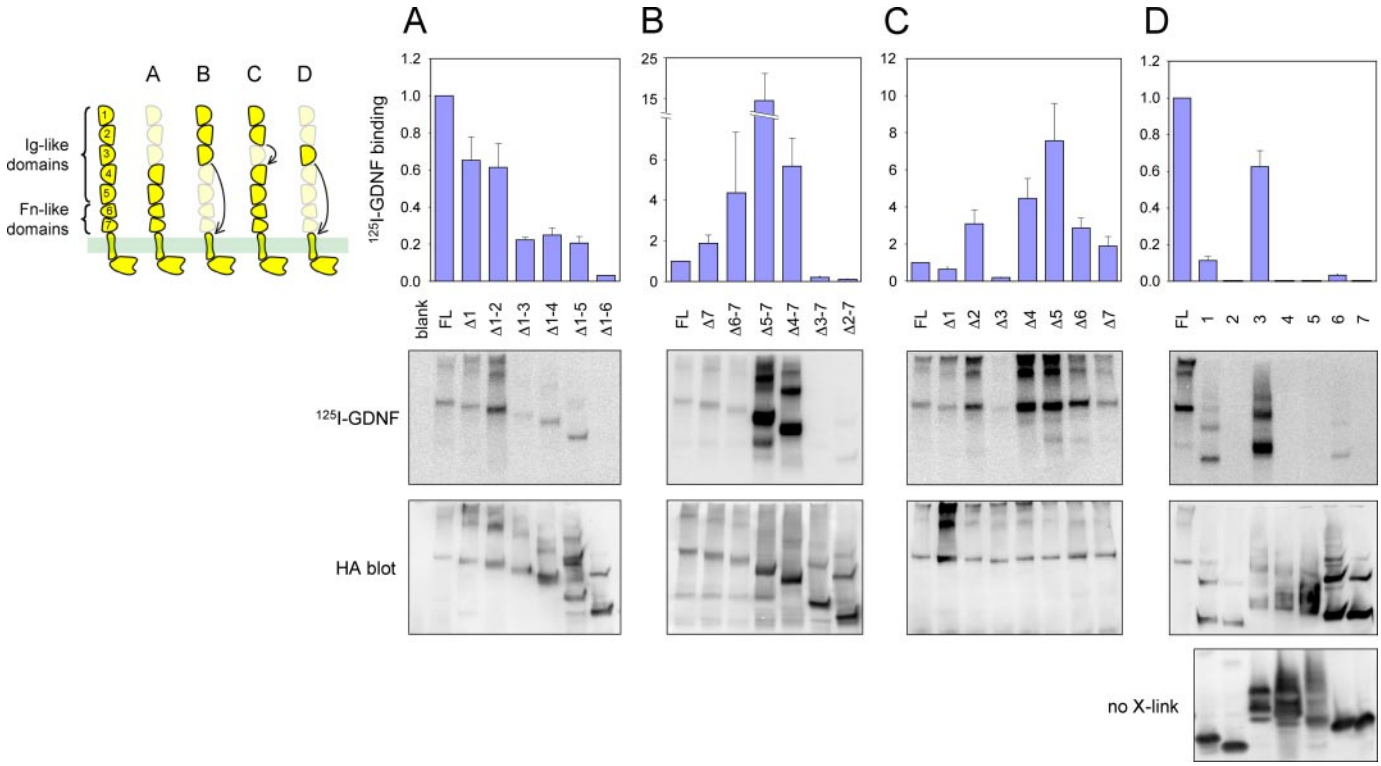

FIGURE 1. **Identification of Ig domain 3 as the necessary and sufficient GDNF binding determinant in NCAM.** Binding of ^{125}I-GDNF to NCAM deletion constructs expressed on the surface of transfected COS cells was analyzed by chemical cross-linking and autoradiography. Blots were subsequently probed with anti-HA antibodies for normalization of binding data. Normalized binding is plotted relative to that of the full-length (*FL*) NCAM molecule as average ± S.E. of three to seven independent experiments. Four deletion series were generated for these experiments (see diagram), deletion of NCAM domains from the N terminus (*A*), deletions from the C-terminal end of the extracellular region (*B*), deletion of single domains (*C*), and single domains on their own (*D*). Cross-linking resulted in the stabilization of higher order interactions between NCAM molecules, also in those carrying single domains, leading to the appearance of additional bands in anti-HA immunoblots. Note that in the absence of cross-linking (*no x-link*), single domain constructs run as a single band, except those carrying glycosylation sites.

Lys^{289}-Tyr^{396}; domain 5, Ala^{397}-Asp^{490}; domain 6, Thr^{491}-Arg^{591}; domain 7, Glu^{592}-Ala^{692}. N-terminal deletion constructs were made by PCR, using *Pfu* DNA polymerase (Promega), with a sense primer corresponding to the beginning of the first domain after the deletion and an antisense primer corresponding to the end of the full-length rat NCAM^{140} cDNA. The sense and antisense primers contained SfiI and NotI restriction sites, respectively. The PCR fragments were digested with SfiI and NotI (New England Biolabs) and ligated into a SfiI/NotI-digested pSecTag 2A Hygro vector (Invitrogen) modified with a hemagglutinin (HA) tag insertion between the secretion tag and the SfiI site. C-terminal deletions (from the C-terminal end of the extracellular region) were made by fusing two PCR fragments. One fragment was made using the full-length sense primer and the antisense primer corresponding to the end of the most C-terminal domain to be present in the final construct (*e.g.* the end of domain 3 in the Δ4–7 construct). The other fragment was made using a sense primer corresponding to the first extracellular juxtamembrane residues following domain 7, together with the full-length antisense primer. The full-length sense and antisense primers contained SfiI and NotI restriction sites, respectively. The two fragments were digested with SfiI or NotI, respectively, and ligated into the SfiI/NotI-digested vector. The ligation site between the two fragments was kept blunt-ended to avoid the introduction of any additional amino acids. Single domain deletions were made similarly to the C-terminal deletions, the difference being that the second fragment was different for all constructs, beginning with the domain immediately 3′ of the one to be deleted (*e.g.* for the Δ3 construct, the second fragment begins with domain 4). Single domains were made in the same way as the N-terminal-truncated constructs but with the appropriate C-terminal deletion construct as a template (*e.g.* Δ5–7 for the "domain 4 only" construct). As pSecTag already contains an efficient signal sequence, the endogenous NCAM signal sequence was excluded from all constructs. The quadruple mutant constructs were made with the "QuikChange Multi" mutagenesis kit (Stratagene) using three primers simultaneously: one targeting both E236A and D242A, another for D250A, and a third for E272A.

Chemical Cross-linking

COS-7 cells grown in Dulbecco's modified Eagle's medium with 10% fetal bovine serum in 100-mm plates were transfected with 15 μg of the appropriate DNA constructs with 2 μg of polyethyleneimine/μg of DNA. Two days after transfection, the plates were washed three times with phosphate-buffered saline (PBS) and incubated with I^{125}-labeled GDNF at a concentration of 20 ng/ml in binding buffer (PBS, 1 mg/ml bovine serum albumin, 1 mg/ml D-glucose, 0.1 mM $CaCl_2$, 0.1 mM $MgCl_2$) for 2 h at 4 °C with gentle rocking. After cross-linking for 45 min with

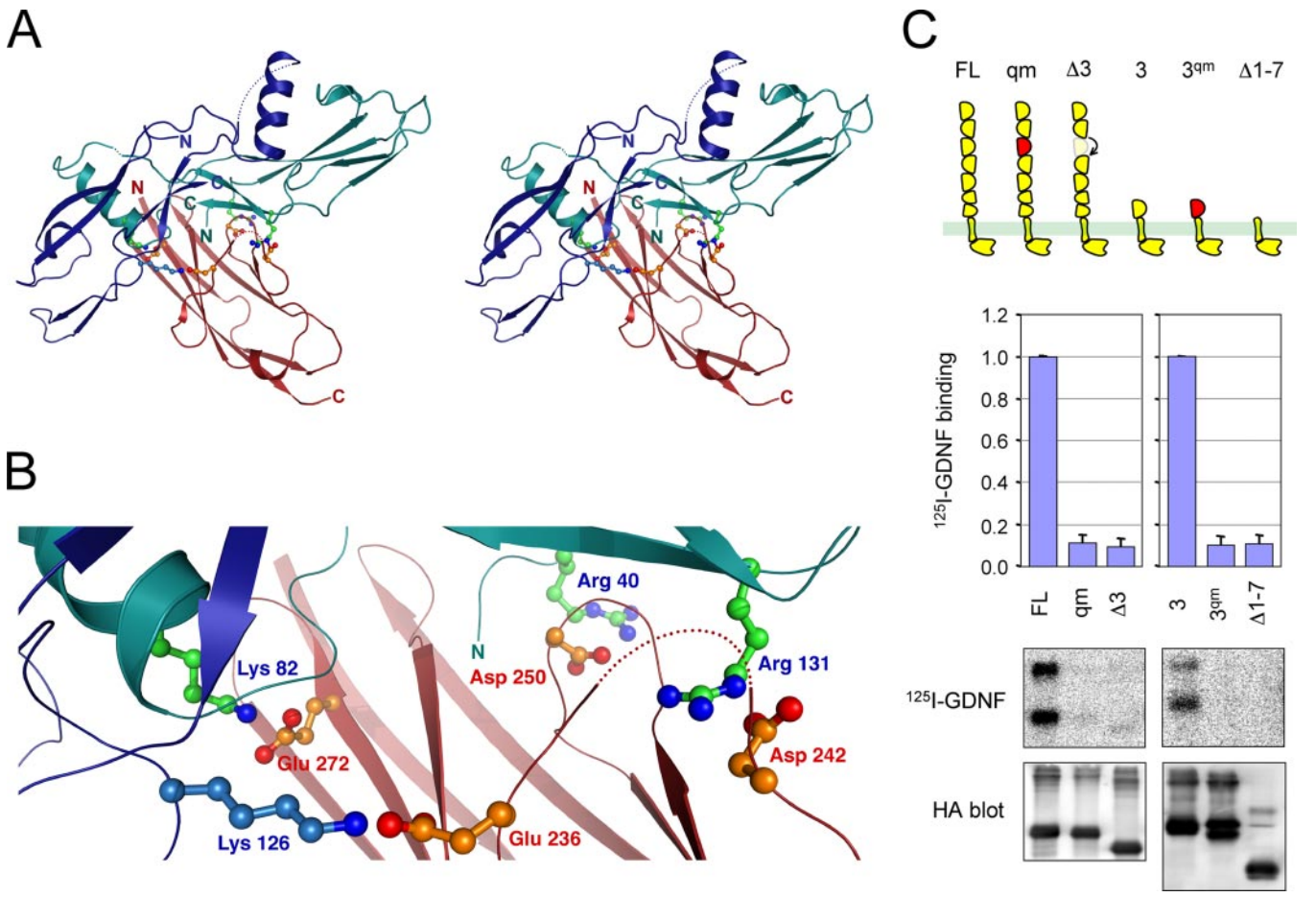

FIGURE 2. **Molecular modeling and functional analysis of candidate residues in the GDNF·NCAM interface.** *A*, stereo view of the docking of NCAM Ig domain 3 and GDNF. Principal residues involved in charged/electrostatic interactions are *highlighted*. N and C termini are indicated. *Dotted lines* connect segments of the GDNF molecule lacking electron density in the crystal structure (21). *B*, close-up view of *panel A* highlighting key residues in the GDNF·NCAM interface. *C*, normalized binding of ^{125}I-GDNF to full-length NCAM (*FL*), quadruple point mutant (*qm*), NCAM lacking domain 3 (Δ*3*), domain 3 alone (*3*), domain 3 with the quadruple point mutation (*3^{qm}*), and NCAM without an extracellular domain (Δ*1–7*).

EDAC/NHS-S (Pierce), plates were quenched with 50 mM glycine and washed three times with PBS.

Selective Immunoprecipitation of Cell Surface Molecules

To normalize GDNF binding to the levels of expression of different constructs at the cell surface, we performed selective immunoprecipitation of cell surface molecules in living cells. Following chemical cross-linking of I^{125}-GDNF, cell monolayers were incubated with 10 μg/ml anti-HA antibodies (clone 12CA5; Roche Applied Science) in binding buffer for 1 h. The plates were then washed six times with PBS and lysed with 0.75 ml of lysis buffer (PBS, 60 mM octyl-β-glucoside, 2 mM EDTA, and protease inhibitors), and cells were collected with a cell lifter. After a 1-h incubation at 4 °C with shaking, lysates were spun for 10 min at 10,000 × *g*, gamma-bind protein G-Sepharose (Amersham Biosciences) was added to the cleared lysates, and the samples were incubated for 1 h with shaking. The immunoprecipitates were washed four times, run on 4–15% gradient SDS-PAGE gels, and transferred to polyvinylidene difluoride membranes. Autoradiographs were scanned in a STORM 840 phosphorimager, and the membranes were subsequently immunoblotted with anti-HA antibodies, developed with Enhanced Chemifluorescence (GE Healthcare), and scanned in a STORM 840. Quantifications were made using ImageQuant 5.2 (GE Healthcare).

Cell Adhesion Assay

Jurkat cells were transfected in 12-well plates with NCAM constructs together with either green fluorescent protein or Ds-Red-encoding plasmids using FuGENE 6 (Roche Applied Science) in 2 ml of complete medium containing 10% fetal calf serum. On the following day, 100 μl each of green fluorescent protein- and Ds-Red-transfected cells were combined and mixed with 100 μl of serum-free medium in 48-well plates. After 48 h of incubation, green cells, red cells, and cell aggregates were quantified under green and red fluorescence illumination on a motorized Axiovert 200 microscope controlled by OpenLab software (Improvision). Cell adhesion was expressed as the percentage of green cells present in clusters that also contained red cells.

Molecular Modeling

Docking—Structures used in molecular simulations were taken from the Protein Data Bank (PDB) with codes 1QZ1 for domains 1–3 of NCAM (28) and 1AGQ (chains A and B) for the GDNF dimer (21). Domain 3 of NCAM was docked to GDNF using Molsoft ICM-Pro 3.2 (Molsoft LLC, La Jolla, CA) with soft potentials, where van der Waals forces have a cut-off value to allow for side chain movements. The resulting complex was subsequently refined by energy minimizations to remove

clashes. Multiple docking calculations were started from 27 evenly distributed positions around GDNF. No limitations, constraints, or biases were invoked on where the two proteins should dock. All dockings consistently yielded the same binding conformation, with the best binding energy of −64.2 kcal/mol. For comparison, NCAM domains 1 and 2 were also docked to GDNF. Docking of domain 1 got significantly worse binding energy (5.2 kcal/mol reduction) compared with domain 3 and was therefore classified as a non-binder. On the other hand, docking of domain 2 resulted in a smaller difference (1.9 kcal/mol reduction) in binding energy compared with domain 3. However, this interaction would cause major clashes between GDNF and the remainder of the NCAM molecule, as the C-terminal end of NCAM domain 2 would directly extend right through the middle of the GDNF dimer. Thus, the docking calculations clearly showed that the best binding was to domain 3, in agreement with our experimental results. We also made a docking calculation of the NCAM domain 3 with the four mutated residues changed to alanines, resulting in a decrease of binding energy of 4.7 kcal/mol. In this analysis, the ranking is important, because the calculated binding energies are only relative. The ranking clearly shows much better binding of domain 3 compared with the mutated domain 3 or domain 1. The coordinates of the docking of NCAM domain 3 and GDNF can be found as a PDB file in the supplemental material available on-line.

Complex Formation—GFRα1 has been shown to bind to the distal poles of the GDNF dimer (25). The crystal structure of a homologous complex between GFRα3 and Artemin has been solved recently (23) (PDB code 2GH0). This complex was used to guide the superposition of GFRα1 onto the GDNF·NCAM complex in order to get a first approximation of the possible architecture of a tripartite complex. The GFRα3 structure (with 44% residue identity to GFRα1) was used as a template for calculating a homology model of GFRα1 using ICM-Pro. The structures of GDNF and Artemin monomers are very similar (root mean square deviation 2.4 Å for the core region, 37% sequence identity) and therefore easily superimposable. However, at the intersubunit interface there are slightly different bending angles. The positioning of GFRα1 in relation to GDNF was obtained by first superimposing the GFRα3·Artemin complex individually onto each GDNF subunit; thereafter, the GFRα1 was superimposed onto GFRα3. In the resulting complex we have not optimized the interface between GFRα1 and GDNF because we only use it as a general estimation of the complex architecture, *i.e.* to judge whether our model of the NCAM-GDNF interaction is compatible with a tripartite complex.

RESULTS AND DISCUSSION

GDNF binding sites in NCAM were investigated by assessing the binding activities of a large collection of NCAM deletion mutants. Four series of NCAM constructs were made carrying (i) progressively larger deletions from the N terminus, (ii) progressively larger deletions from the C-terminal end of the extracellular region, (iii) single domains deleted, or (iv) single domains on their own, all containing the native transmembrane and intracellular domains of the $p140^{NCAM}$ isoform (Fig. 1, *A–D*). As each domain of the NCAM extracellular region is encoded by two consecutive exons in the *Ncam* gene (30), we used the exon-intron structure to define domain boundaries (see "Experimental Procedures" for details). Following equilibrium binding of ^{125}I-GDNF and chemical cross-linking, NCAM molecules present at the cell surface were selectively immunoprecipitated from their

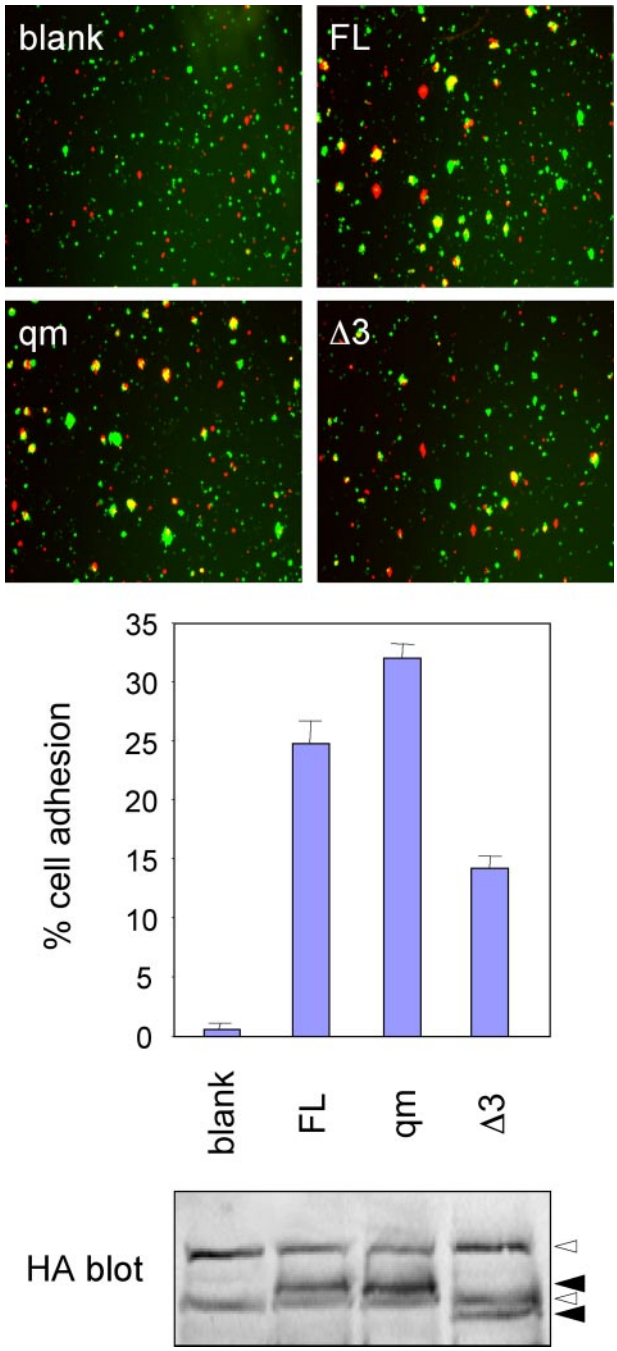

FIGURE 3. **Disruption of GDNF-NCAM interactions does not affect NCAM-mediated cell adhesion.** Assay of homophilic cell adhesion in Jurkat cells transfected with a control plasmid (*blank*) or the indicated NCAM constructs. Percentage cell adhesion refers to the proportion of green cells present in mixed cell aggregates. Data are presented as average ± S.D. ($n = 4$). Comparable levels of NCAM expression in Jurkat cells were confirmed by anti-HA immunoblotting (*solid arrowheads* in *bottom panel*; *smaller open arrowheads* denote unspecific bands).

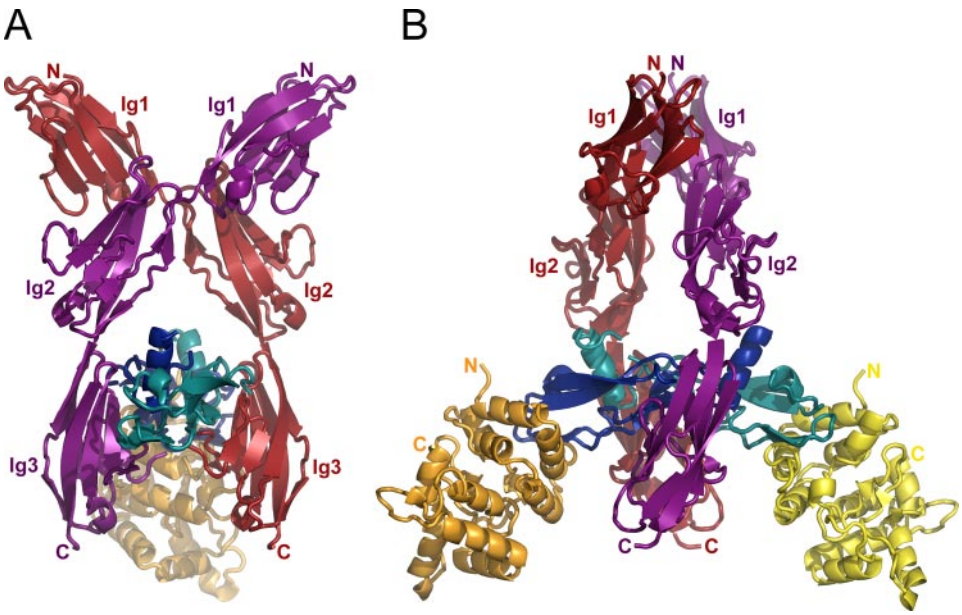

FIGURE 4. **Model of a tripartite complex between GDNF, NCAM, and GFRα1.** *A* and *B*, orthogonal views of a model of the 2:2:2 complex between GDNF (*blue*) (21), NCAM domains 1–3 (*red*) (28), and the ligand binding domain of GFRα1 (*yellow*) (modeled from Ref. 23). N and C termini of NCAM and GFRα1 are indicated (the termini of GDNF are buried in the complex and could not be labeled). For clarity, one GFRα1 domain was removed from the foreground in *panel A*.

N-terminal HA tag, fractionated by SDS/PAGE, and subjected to autoradiography and HA immunoblotting.

Analysis of the N-terminal deletion series revealed a major reduction in GDNF binding after deletion of the third Ig domain (Fig. 1*A*). The importance of this domain for GDNF binding was also apparent from the binding activities of the C-terminal deletion series, in which only constructs containing this domain were capable of binding ligand (Fig. 1*B*). Intriguingly, constructs lacking Ig domains 4 or 5 (*i.e.* Δ5–7 and Δ4–7) displayed increased GDNF binding compared with the full-length molecule (Fig. 1*B*). The bulk of glycosylation sites are present in these domains (31, 32), suggesting that NCAM glycosylation negatively affects GDNF binding.

The requirement of individual domains for ligand binding was further investigated by deleting single domains from the NCAM molecule. Only deletion of the third domain affected the ability of NCAM to bind GDNF, indicating its requirement for ligand binding (Fig. 1*C*). Deletion of either domains 4 or 5 again increased GDNF binding, indicating a negative effect of these heavily glycosylated domains on ligand interaction. Finally, the sufficiency of individual NCAM domains for GDNF binding was assessed using constructs carrying single domains as the sole extracellular region of the molecule (Fig. 1*D*). Domain 3 was found to bind GDNF very well on its own, whereas other domains bound weakly or not at all. Together, the results from our deletion analyses show that the third Ig domain of NCAM is both necessary and sufficient for GDNF binding and therefore represents the principal ligand binding determinant in this receptor.

Using the crystal structures of GDNF (21) and NCAM domain 3 (28), we modeled the interaction between the two molecules with the molecular modeling program ICM-Pro 3.2. An unbiased docking calculation was obtained by starting from 27 different, evenly distributed positions around the GDNF molecule, thus sampling all possible interaction sites. Six of these yielded the highest ranking docking conformations, as judged by their calculated binding energies, all of which placed NCAM domain 3 on the cleft between the two protomers of the GDNF dimer (Fig. 2*A*), and involved identical residues in the contact of the two molecules. The interface is dominated by electrostatic interactions, with four residue pairs having distances between 2.9 and 3.5 Å, Arg^{40}, Lys^{82}, and Arg^{131} from the first GDNF protomer and Lys^{126} from the second, pairing with Asp^{250}, Glu^{272}, Asp^{242}, and Glu^{236}, respectively, from NCAM domain 3 (Fig. 2*B*). Mutation of these four acidic residues in the ligand binding interface of NCAM domain 3 to alanine abolished the ability of this domain to bind GDNF in cross-linking assays (Fig. 2*C*). When introduced in the full-length NCAM molecule, the quadruple mutation (*qm*) reduced GDNF binding to background levels, phenocopying the effects of deletion of domain 3 (Fig. 2*C*). In addition to bringing experimental support to our model of the GDNF·NCAM complex, these results identify four specific residues within the 665-residue-long NCAM extracellular domain that are specifically required for its ability to interact with GDNF.

Most models of NCAM homophilic interaction agree on the requirement of domain 3 for efficient NCAM-mediated cell adhesion (28, 33–35). We therefore tested the effects of mutations that disrupt GDNF binding on the ability of NCAM to mediate homophilic cell-cell interactions. Cells grown in suspension were transfected with different NCAM constructs along with expression plasmids for either green or red fluorescent proteins and tested for their ability to form mixed aggregates containing green and red cells. Whereas full-length NCAM readily induced the formation of cell aggregates in this assay, deletion of domain 3 diminished the ability of the molecule to promote cell adhesion by ~50% (Fig. 3). Domain 3 on its own displayed no adhesive properties in this assay (data not shown). In contrast, the quadruple point mutant of NCAM retained wild type levels of cell adhesion (Fig. 2*D*), indicating that the four residues that are critical for GDNF binding are not involved in NCAM homophilic interactions. More generally, this result demonstrates that the two NCAM activities can be genetically dissociated and provides the opportunity to test their *in vivo* relevance through, for example, the generation of mice carrying the $Ncam^{qm}$ allele.

Because of the 2-fold symmetry of the GDNF dimer, we asked whether the GDNF·NCAM interface we identified may allow the formation of NCAM dimers bound to the same GDNF molecule. Two NCAM molecules (*i.e.* domains 1–3)

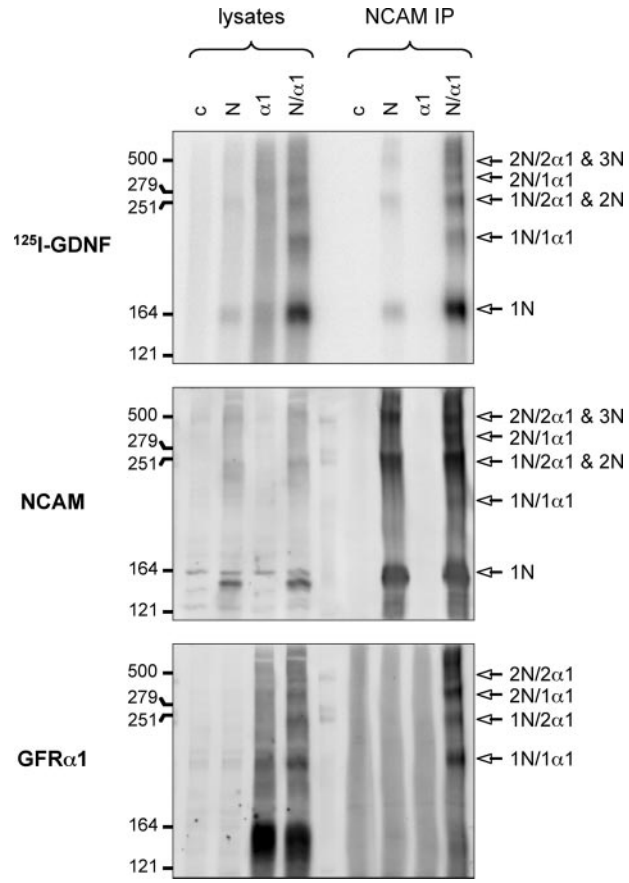

FIGURE 5. **Recovery of a tripartite complex between GDNF, NCAM, and GFRα1 by chemical cross-linking.** Biochemical analysis of complex formation between ^{125}I-GDNF, HA-tagged NCAM (*N*), and Myc-tagged GFRα1 (*α1*). The *upper panel* shows an autoradiogram, and the *middle* and *bottom panels* show reprobing of the same membrane with HA and Myc antibodies, respectively. The deduced stoichiometry and composition of cross-linked complexes are shown to the right. As previously reported (12), co-expression with GFRα1 enhanced GDNF binding to NCAM. However, the complex labeled 1N/1α1 was still invisible in the NCAM-only lane (*N*) after strong overexposure of the autoradiogram (not shown). The two strong bands at the bottom of the GFRα1 blot correspond to GFRα1 dimers.

could be arranged around a GDNF dimer, each binding to symmetrically related interfaces on opposite sides (Fig. 4*A*). Interestingly, this configuration was almost identical to the one previously proposed for cis-interacting NCAM dimers based on the crystal structure of domains 1–3 (28) (compare with Fig. 2*A* from Ref. 28), suggesting that it may represent a *bona fide* conformation for GDNF binding.

We then asked whether our model of the GDNF·NCAM complex was compatible with the association of GFRα1 to GDNF. Previous structure-function studies have localized the GFRα1 binding site to the two poles of the elongated GDNF dimer (25), away from the NCAM binding interface, a notion that has recently been confirmed by the crystal structure of the GDNF homolog Artemin in complex with the ligand binding domain of its cognate GFRα3 receptor (23). Using the coordinates of that complex, we modeled the interaction between GDNF and the ligand binding fragment of GFRα1. Based on this model, two GFRα1 molecules, one at each end of the GDNF dimer, could be positioned onto the GDNF·NCAM model to form a 2:2:2 complex containing the three proteins (Fig. 4, *A* and *B*). Although GFRα1 and NCAM are known to interact with each other (12), no such interaction can be observed in the model, suggesting that it may be mediated by other domains in the NCAM molecule. It should be noted that this model would place the C termini of the GDNF binding domains of GFRα1 and NCAM in opposite directions, leaving open the possible orientation of this complex relative to the plasma membrane. Importantly, however, the topologies of full-length GFRα1 and NCAM are unlikely to be straight rods perpendicular to the plasma membrane. Thus, although it has been suggested that the C terminus of the ligand binding domain of GFRα3 points toward the membrane (23), both N and C termini in this domain are on the same side of the structure, where an additional 150-residue-long N-terminal domain still needs to be accommodated. In the case of NCAM, earlier electron microscopy studies have indicated a heavily kinked conformation of its extracellular domain (36, 37).

To obtain evidence for the existence of a tripartite complex between GDNF, NCAM, and GFRα1, we performed chemical cross-linking and immunoprecipitation studies in cells transfected with expression constructs carrying HA-tagged NCAM and Myc-tagged GFRα1. Following ^{125}I-GDNF binding and cross-linking, several complexes could be recovered after immunoprecipitation with anti-HA antibodies (thus containing NCAM) that could be visualized by autoradiography (thus containing GDNF) and that also reacted with anti-Myc antibodies (thus containing GFRα1) (Fig. 5). For example, a complex containing one molecule each of GDNF, NCAM, and GFRα1 (labeled *1N/1α1* in Fig. 5) could be specifically detected after NCAM immunoprecipitation and only in cells that received both NCAM and GFRα1 (Fig. 5). Moreover, complexes corresponding to the size of the tripartite 2:2:2 complex modeled in Fig. 4, *A* and *B*, could also be detected (Fig. 5, *2N/2α1*). Because of multiple NCAM cis and trans interactions, this complex run at the same molecular weight as that of three NCAM molecules cross-linked together (Fig. 5, *3N*).

In conclusion, we have identified a localized and specific binding determinant in NCAM that is crucial for its interaction with GDNF, dispelling a role for the adhesive or otherwise "sticky" properties of NCAM in GDNF binding. We have also demonstrated that ligand binding and cell adhesion can be genetically dissociated and provided the first insights into the molecular architecture of a multicomponent GDNF receptor.

REFERENCES

1. Barker, R. A. (2006) *Lancet Neurol.* **5,** 285–286
2. Gill, S. S., Patel, N. K., Hotton, G. R., O'Sullivan, K., McCarter, R., Bunnage, M., Brooks, D. J., Svendsen, C. N., and Heywood, P. (2003) *Nat. Med.* **9,** 589–595
3. Gardell, L. R., Wang, R., Ehrenfels, C., Ossipov, M. H., Rossomando, A. J., Miller, S., Buckley, C., Cai, A. K., Tse, A., Foley, S. F., Gong, B., Walus, L., Carmillo, P., Worley, D., Huang, C., Engber, T., Pepinsky, B., Cate, R. L., Vanderah, T. W., Lai, J., Sah, D. W., and Porreca, F. (2003) *Nat. Med.* **9,** 1383–1389
4. Jing, S. Q., Wen, D. Z., Yu, Y. B., Holst, P. L., Luo, Y., Fang, M., Tamir, R., Antonio, L., Hu, Z., Cupples, R., Louis, J. C., Hu, S., Altrock, B. W., and Fox, G. M. (1996) *Cell* **85,** 1113–1124
5. Treanor, J., Goodman, L., Desauvage, F., Stone, D. M., Poulsen, K. T., Beck, C. D., Gray, C., Armanini, M. P., Pollock, R. A., Hefti, F., Phillips, H. S., Goddard, A., Moore, M. W., Buj-Bello, A., Davies, A. M., Asai, N., Takahashi, M.,

Vandlen, R., Henderson, C. E., and Rosenthal, A. (1996) *Nature* **382,** 80–83
6. Baloh, R. H., Tansey, M. G., Golden, J. P., Creedon, D. J., Heuckeroth, R. O., Keck, C. L., Zimonjic, D. B., Popescu, N. C., Johnson, E. M., and Milbrandt, J. (1997) *Neuron* **18,** 793–802
7. Baloh, R. H., Gorodinsky, A., Golden, J. P., Tansey, M. G., Keck, C. L., Popescu, N. C., Johnson, E. M., and Milbrandt, J. (1998) *Proc. Natl. Acad. Sci. U. S. A.* **95,** 5801–5806
8. Trupp, M., Raynoschek, C., Belluardo, N., and Ibáñez, C. F. (1998) *Mol. Cell. Neurosci.* **11,** 47–63
9. GFRα Nomenclature Committee (1997) *Neuron* **19,** 485
10. Durbec, P., Marcos-Gutierrez, C. V., Kilkenny, C., Grigoriou, M., Suvanto, P., Wartiovaara, K., Smith, D., Ponder, B., Costantini, F., Saarma, M., Sariola, H., and Pachnis, V. (1996) *Nature* **381,** 789–792
11. Trupp, M., Arenas, E., Fainzilber, M., Nilsson, A.-S., Sieber, B. A., Grigoriou, M., Kilkenny, C., Salazar-Grueso, E., Pachnis, V., Arumäe, U., Sariola, H., Saarma, M., and Ibáñez, C. F. (1996) *Nature* **381,** 785–789
12. Paratcha, G., Ledda, F., and Ibáñez, C. F. (2003) *Cell* **113,** 867–879
13. Airaksinen, M. S., and Saarma, M. (2002) *Nat. Rev. Neurosci.* **3,** 383–394
14. Taraviras, S., Marcos, G. C., Durbec, P., Jani, H., Grigoriou, M., Sukumaran, M., Wang, L. C., Hynes, M., Raisman, G., and Pachnis, V. (1999) *Development* **126,** 2785–2797
15. Natarajan, D., Marcos-Gutierrez, C., Pachnis, V., and de Graaff, E. (2002) *Development* **129,** 5151–5160
16. Sainio, K., Suvanto, P., Davies, J., Wartiovaara, J., Wartiovaara, K., Saarma, M., Arumae, U., Meng, X. J., Lindahl, M., Pachnis, V., and Sariola, H. (1997) *Development* **124,** 4077–4087
17. de Graaff, E., Srinivas, S., Kilkenny, C., D'Agati, V., Mankoo, B. S., Costantini, F., and Pachnis, V. (2001) *Genes Dev.* **15,** 2433–2444
18. Ledda, F., Paratcha, G., Sandoval-Guzmán, T., and Ibáñez, C. F. (2007) *Nat. Neurosci.* **10,** 293–300
19. Paratcha, G., Ibáñez, C. F., and Ledda, F. (2005) *Mol. Cell Neurosci.* **31,** 505–514
20. Iwase, T., Jung, C. G., Bae, H., Zhang, M., and Soliven, B. (2005) *J. Neurochem.* **94,** 1488–1499
21. Eigenbrot, C., and Gerber, N. (1997) *Nature Struct. Biol.* **4,** 435–438
22. Leppanen, V. M., Bespalov, M. M., Runeberg-Roos, P., Puurand, U., Merits, A., Saarma, M., and Goldman, A. (2004) *EMBO J.* **23,** 1452–1462
23. Wang, X., Baloh, R. H., Milbrandt, J., and Garcia, K. C. (2006) *Structure* **14,** 1083–1092
24. Baloh, R. H., Tansey, M. G., Johnson, E. M., and Milbrandt, J. (2000) *J. Biol. Chem.* **275,** 3412–3420
25. Eketjäll, S., Fainzilber, M., Murray-Rust, J., and Ibáñez, C. F. (1999) *EMBO J.* **18,** 5901–5910
26. Scott, R. P., and Ibáñez, C. F. (2001) *J. Biol. Chem.* **276,** 1450–1458
27. Anders, J., Kjær, S., and Ibáñez, C. F. (2001) *J. Biol. Chem.* **276,** 35808–35817
28. Soroka, V., Kolkova, K., Kastrup, J. S., Diederichs, K., Breed, J., Kiselyov, V. V., Poulsen, F. M., Larsen, I. K., Welte, W., Berezin, V., Bock, E., and Kasper, C. (2003) *Structure* **11,** 1291–1301
29. Small, S. J., Shull, G. E., Santoni, M. J., and Akeson, R. (1987) *J. Cell Biol.* **105,** 2335–2345
30. Owens, G. C., Edelman, G. M., and Cunningham, B. A. (1987) *Proc. Natl. Acad. Sci. U. S. A.* **84,** 294–298
31. Albach, C., Damoc, E., Denzinger, T., Schachner, M., Przybylski, M., and Schmitz, B. (2004) *Anal. Bioanal. Chem.* **378,** 1129–1135
32. Liedtke, S., Geyer, H., Wuhrer, M., Geyer, R., Frank, G., Gerardy-Schahn, R., Zahringer, U., and Schachner, M. (2001) *Glycobiology* **11,** 373–384
33. Atkins, A. R., Gallin, W. J., Owens, G. C., Edelman, G. M., and Cunningham, B. A. (2004) *J. Biol. Chem.* **279,** 49633–49643
34. Johnson, C. P., Fujimoto, I., Perrin-Tricaud, C., Rutishauser, U., and Leckband, D. (2004) *Proc. Natl. Acad. Sci. U. S. A.* **101,** 6963–6968
35. Wieland, J. A., Gewirth, A. A., and Leckband, D. E. (2005) *J. Biol. Chem.* **280,** 41037–41046
36. Becker, J. W., Erickson, H. P., Hoffman, S., Cunningham, B. A., and Edelman, G. M. (1989) *Proc. Natl. Acad. Sci. U. S. A.* **86,** 1088–1092
37. Hall, A. K., and Rutishauser, U. (1987) *J. Cell Biol.* **104,** 1579–1586